

Article

Not peer-reviewed version

---

# Analysis of the 2022 El Tejado Ravine Mudflow (Quito, Ecuador) from the Sedimentological and the Published Multimedia Documents Approach

---

Liliana Troncoso , [Francisco Javier Torrijo Echarri](#) <sup>\*</sup> , Elias Ibadango , Luis Pilatasig , Olegario Alonso-Pandavenes , [Alex Mateus](#) , Stalin Solano , Ruber Cañar , Nicolás Rondal , [Francisco Viteri](#)

Posted Date: 23 April 2024

doi: 10.20944/preprints202404.1489.v1

Keywords: mudflow; El Tejado ravine; sedimentology; La Gasca Street; Pichincha volcano; multimedia



Preprints.org is a free multidiscipline platform providing preprint service that is dedicated to making early versions of research outputs permanently available and citable. Preprints posted at Preprints.org appear in Web of Science, Crossref, Google Scholar, Scilit, Europe PMC.

Copyright: This is an open access article distributed under the Creative Commons Attribution License which permits unrestricted use, distribution, and reproduction in any medium, provided the original work is properly cited.

*Article*

# Analysis of the 2022 El Tejado Ravine Mudflow (Quito, Ecuador) from the Sedimentological and the Published Multimedia Documents Approach

Liliana Troncoso <sup>1</sup>, Francisco Javier Torrijo Echarri <sup>2\*</sup>, Elias Ibadango <sup>1</sup>, Luis Pilatasig <sup>1</sup>, Olegario Alonso-Pandavenes <sup>1</sup>, Alex Mateus <sup>1</sup>, Stalin Solano <sup>1</sup>, Ruber Cañar <sup>1</sup>, Nicolás Rondal <sup>1</sup> and Francisco Viteri <sup>1</sup>

<sup>1</sup> Universidad Central del Ecuador. FIGEMPA Faculty; lptroncoso@uce.edu.ec (L.T.); ceibadango@uce.edu.ec (E.I.); lfpilatasig@uce.edu.ec (L.P.); omaloso@uce.edu.ec (O.A.-P.); ammateus@uce.edu.ec (A.M.); spsolano@uce.edu.ec (S.S.); rdcanar@uce.edu.ec (R.C.); narondal@uce.edu.ec (N.R.); frviteri@uce.edu.ec (F.V.)

<sup>2</sup> Department of Geotechnical Engineering, Research Centre for Architecture, Heritage and Management for Sustainable Development (PEGASO), Universitat Politècnica de València, Camino de Vera s/n, 46022 Valencia, Spain

\* Correspondence: fratorec@trr.upv.es

**Abstract:** On the afternoon of January 31, 2022, the northwest and central part of the city of Quito (Ecuador) was hit by a mud-flow that originated in one of the ravines of the Pichincha volcanic complex. According to the official reports, there were 28 fatalities, one missing person, 52 injured, and 53 families affected. The mudflow was triggered by unusual and heavy rainfall in the upper part of the drainage. However, the analysis of the deposits allowed us to establish the existence of anthropogenic elements as crucial components of a local disaster that affected daily life in the city for more than a week. Based on the preliminary data, we were able to determine that the mud and water flowed through different streets of the city, reaching a maximum distance of 3.2 km from the overflow point (collector, construction works to dam the drainage under the city). The analysis of the multimedia material published on social networks and in the press also made it possible to detect the change in the behavior of the flow during its evolution, which went from a hyper-concentrated flow to muddy water. A similar event occurred in 1975, and although it was a larger event (52000 m<sup>3</sup>, seven times larger than in 2022), it caused two deaths and little damage in the same area. The main causes of the disaster included urban development that did not meet the needs of the area and a lack of awareness or ignorance about the management and intervention of drainage in Quito City.

**Keywords:** mudflow; El Tejado ravine; sedimentology; La Gasca Street; Pichincha volcano; multimedia

## 1. Introduction

A broad compression of the term mudflow denotes the motion of a mixture of sediment particles and other materials in an aqueous media, i.e., a multi-phase component where the water controls the movement [1]. The solid phase can include sediment grains in various sizes and compositions (mostly in percentage) and vegetation flowing down from a high area through narrow or channel-confined shapes (ravines or valleys), and gravity is the force that gives energy to the flow. The typical trigger is the heavy rains over the high level of the hydrogeological basin [1–3].

The energy developed in that kind of event depends on the potential energy (changes in elevation from head to toe of the flow) but always has a destructive power, sometimes very high, and

can produce loss of human lives, damage, and modify topography. Of course, when that kind of phenomenon impacts an urbanized area, the losses can increase and cause a disaster [3].

The urban area of the Metropolitan District of Quito (MDQ), the capital of Ecuador, is located in a basin raised at 2800 m. a. s. l., to the west of the so-called Interandean Valley. It was developed in a geological context marked by the presence of the slopes associated with the Pichincha Volcanic Complex (PVC) to the west, and a series of hills that are the expression of a system of reverse faults called the Quito Fault System (to the east) [4].

In the western urban limit of the MDQ, about 85 streams [5] are present, fed by the runoff water from the PVC. Throughout the history and development of the city, they have been replaced or modified by fills or sewers [6]. The city and the citizens' relationship with the streams has been complex because they are used as sites for garbage disposal and accumulation of debris. The lack of public policies or compliance with them has allowed a high degree of exposure in residential areas to phenomena linked to the evolution and functioning of streams, such as mass movements, subsidence, mudflows, and floods, among others. Since the 20th century, the impact of mudflows on sites related to human-intervened drainages has been documented in Quito's written press. One of the most remembered is the mudflow or *aluvión* (used in Ecuador as a local term) of La Gasca (Quito central residential sector related to the whole study area) on February 25, 1975, with an approximate volume of 52000 m<sup>3</sup>. It left a thickness of 20 to 50 cm, which mobilized debris, metric-sized blocks, and tree-cutting fragments, resulting in two deaths, partial destruction of several buildings, vehicles, and damage to roads in the sector [7].

According to [8], since 1996, the Metropolitan Public Company of Drinking Water and Sanitation of Quito (Spanish acronym: EPMAPS) has been responsible for reducing the risk of floods, landslides, and mudslides through plans and projects that integrate the management of the slopes of PVC. These actions were carried out with the help of loans from the Inter-American Development Bank (IDB) and allowed the construction of engineering works to protect river beds. In a report issued by the EPMAPS in 2022, for the event of January 31 of that year, it is noted that between 1997 and 2000, the "*Pichincha Hillsides Protection Program*" was executed, which built 48 control structures (dams, reservoirs, transfer tunnels, catchment structures) in 33 streams on the Pichincha hillsides [9].

Since 2019, the city began to face again the direct impact of mud flows generated in the intervened drains on the slopes of Pichincha, with the case with the most significant impact due to the number of fatalities (more than 20) being that which occurred on the afternoon from January 31, 2022.

This study aims to analyze the mudflow behavior from the sedimentology point of view and across the media publications (from newspapers, affected people, and the net).

## 2. Geographical Location and Previous Knowledge

The urban area of Metropolitan District of Quito (MDQ) is the capital of the Ecuador Republic and the second most populated city (1,91 million people, INEC, 2017, <https://www.ecuadorencifras.gob.ec>). It is located in a longitudinal basin of 37 km in length and 6 km wide (on average) and at 2800 meters above sea level (m.a.s.l.) in the so-called Interandean Valley (Figure 1).

The geological context was marked by the presence of the PVC (the Guagua and Rucu Pichincha volcanoes) just at the west and close to the center area of the city. The volcanic cones have steeper slopes facing the east and are limited by the east by a series of hills expressing a system of reverse faults.

In the western urban limit of the MDQ, about 85 streams and ravines (locally called *quebradas*) are fed by runoff water from that Pichincha volcanic complex. Throughout the history and development of the city, they have been replaced or modified by fills or sewers [10–12].



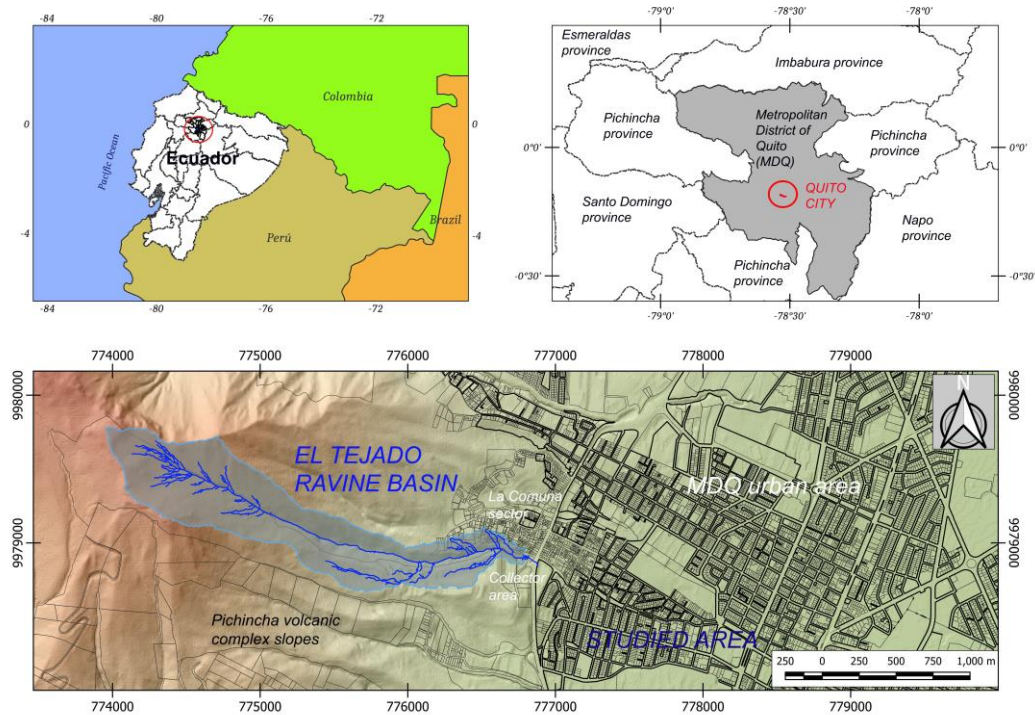


**Figure 1.** Situation map of the study area. Modified from [13].

On Monday, January 31, 2022, between 6:00 PM [14] and 6:30 PM [15], local time, a mudflow was reported that overflowed the catchment structure (sewage collector) at the actual end of the El Tejado ravine in the urban boundary of the MDQ (Figure 2).

The videos from the surveillance cameras of the ECU-911 (the National Integrated Security System) from two intersections: La Gasca Avenue and Francisco Viteri Street and La Gasca Avenue and America Avenue, indicate that the arrival time of the flow front at the América Avenue (an NE-SW main communication axis of the city) was at 6:38 PM.



**Figure 2.** The mudflow crossing the Nuñez de Bonilla Street (A), picture extracted from ECU-911 video footage surveillance camera. Detail of the remained mud on the sewage collector at the end of the El Tejado stream after the mudflow pass. January 31, 2022 (B), obtained from [16].

According to a published video on the social network TikTok (www.tiktok.com), it is suggested that an hour before the overflow occurred, the clogging of the collector of the El Tejado stream was reported [17].

This event caused damage to people, buildings, public goods, essential services, and road infrastructure. According to the National Risk and Emergency Management Service (Spanish acronym SNGRE), the event caused 28 people to die, one missing person, 52 injured, 170 people affected, 53 families affected, seven buildings destroyed, 41 buildings semi-destroyed, 60 public property destroyed (poles electricity and garbage containers), 18 public assets affected (Community Police Unit with patrol cars and motorcycles), private vehicles destroyed and affected (vehicles and motorcycles) and closure of several roads due to the emergency [18].

In the report prepared by the Technical Commission of the Central University of Ecuador for analysis of the event, it is noted that from Friday, January 28 to Monday, January 31, 2022, heavy rainfall was reported that caused soil saturation and increased runoff. Water infiltration caused landslides on the slopes of the channel in the upper part of the El Tejado ravine [19]. According to the Special Meteorological Bulletin of January 31 (obtained on-line the same day from <https://www.inamhi.gob.ec/informacion-en-linea/>; INAMHI government institute), it was noted that the rainfall in January 2022 was 32% greater than that of January 2021 and was 31% above the average values for a traditional January [14].

The study area is located in Quito's north-central and western sectors, in the Belisario Quevedo urban parish (Figure 3). It includes the sectors called Comuna de Santa Clara de San Millán (also named as La Comuna) and La Gasca and focuses on the streets and avenues affected by the direct impact of the flood of January 31, 2022; that is, from the pluvial sewage collector construction on Fulgencio Araujo Street to 6 de Diciembre Avenue (in the NW-SE direction) and from Núñez de Bonilla Street to Indoamérica Square (in the N-S direction).

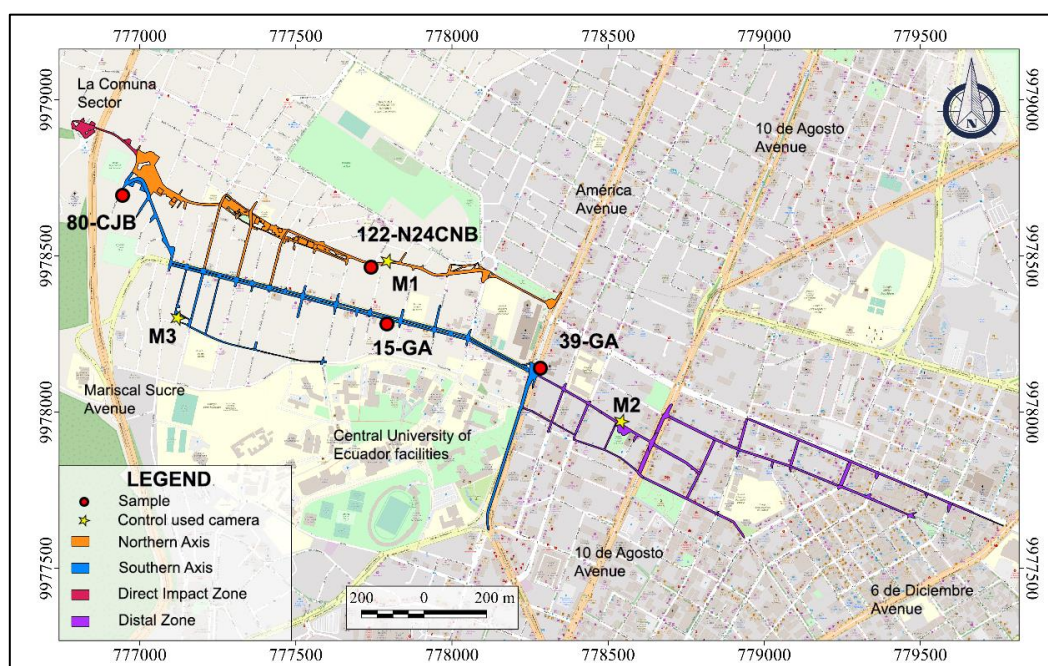


**Figure 3.** Mudflow spread area from the first occurrence, the collector (NW) to the end of the flow in the 6 de Diciembre Avenue (SE). Modified from [17] using a base-map from Spanish version of [13].

The urban neighborhoods affected by the 2022 event are La Comuna, Pambachupa, La Gasca, La Colón, Santa Clara, and La Mariscal. It had a severe affectation on sectors of La Comuna and La Gasca in the upper part, causing loss of lives and personal and real property, high affectation in La Gasca and Pambachupa, causing accumulation of mud and debris on the main avenues and intersections. Less impact was caused in Santa Clara and La Mariscal sectors (América, Cristóbal Colón, Amazonas and 10 de Agosto Avenues, and Alonso de Mercadillo, General Ulpiano Páez, Luis



Cordero, 9 de Octubre, and Diego de Almagro Streets), causing accumulation of sludge and clogging of the sewage system [14].

3. Methodology and Modelizations

3.1. Video, Image and Visual Media Approach

The methodology used in this study has been based on multimedia material (images and videos) related to the mudflow. The information obtained, ordered, and categorized (coding) is a compilation of images and videos from social networks such as Facebook, (www.facebook.com), YouTube (www.youtube.com), TikTok (www.tiktok.com), Instagram (www.instagram.com), and Twitter/X (www.twiiter.com), digital press (television channels and digital newspapers and the ECU-911) [20].

The treatment of the information was divided into a detailed analysis of the videos and images to determine their spatial location (using fixed reference objects, see an example in Figure 4A,B) and temporal location (from four videos with time shown; see Table 1, and Figure 4C).

In the second stage, the kinematic parameters of the mudflow were defined through a detailed field survey of the areas selected from the videos, and these parameters were calculated using the Fudaa-LSPIV software (v. 1.9.2) [21].



**Figure 4.** Observations applying reference points for spatial localization (left image): (A) Panoramic picture from Google Map-Street View [13], and (B) the same frame from 21-GA video footage (ECU-911 video surveillance camera). Identification points: wall painting (a), lighting pole (b), and advertising pole (c). Temporal identification (C): It was obtained from 15-GA video (ECU-911 video surveillance camera), where it can be seen the record of the mudflow, showing the address, local time, and date (red rectangles) [20].

**Table 1.** Temporal location of videos and their position. Modified from [20].

Used code	Adress	Local time	Length
80-CJB	José Berrutieta Street (corner)	18:09:10 PM	13
122-N24CNB	Núñez de Bonilla Avenue crossing García Dec	18:29:10 PM	4

15-GA	La Gasca Avenue crossing Francisco Viteri Street	18:39:37 PM	52
39-GA	La Gasca Avenue crossing América Avenue	18:39:50 PM	49

Two hundred sixty-one multimedia files were handled: 151 videos were in *MP4* format, and 110 images were in *JPG* format throughout the affected area.

The multimedia files sources were searched using free access software tools: InVID-Project (<https://www.invid-project.eu/>), and Google Lens (<https://lens.google/intl/es-419/>), which allows for determining the different websites where the multimedia records of the event were uploaded and shared. That procedure aims to eliminate (debug) the fake videos from database (those that are not actual or of the event), validate them and gain in accuracy.

In calculating the kinematic parameters (surface velocities, average velocity, and caudal flow), a methodology was used based on the study between specific points of the digital video frames of the debris flows. [22,23]. This technique allows a precise evaluation of the dynamic characteristics of debris flows, thus facilitating the understanding of their behavior and potential impact.

It consists of determining the spatial (two-dimensional) coordinates of selected features and objects from pixels identified in video images. The average velocity of the flow surface between two video frames is then calculated as the ratio of the distance traveled to the elapsed time, according to the adapted velocity for video frames (Equation (1)):

$$v = \frac{d \cdot V_{\text{fot}}}{N_{\text{fot}}} \quad (1)$$

Where,  $v$  is the surface speed (m/s),  $d$  is the distance traveled (m),  $V_{\text{fot}}$  is the recording speed of frames ( $\text{s}^2$ ) and  $N_{\text{fot}}$  is the number of frames in the video [22].

Furthermore, the LSPIV (Large Scale Particle Image Velocimetry) technique was applied for good-quality videos of recordings in along-channel flow events (see Figure 5) [24–26]. Due to the development of software and programming, the technique applies to videos recorded from fixed digital cameras, and in recent years, it has been adapted for implementation to videos filmed by the public and shared by different social networks, obtaining good results [24].

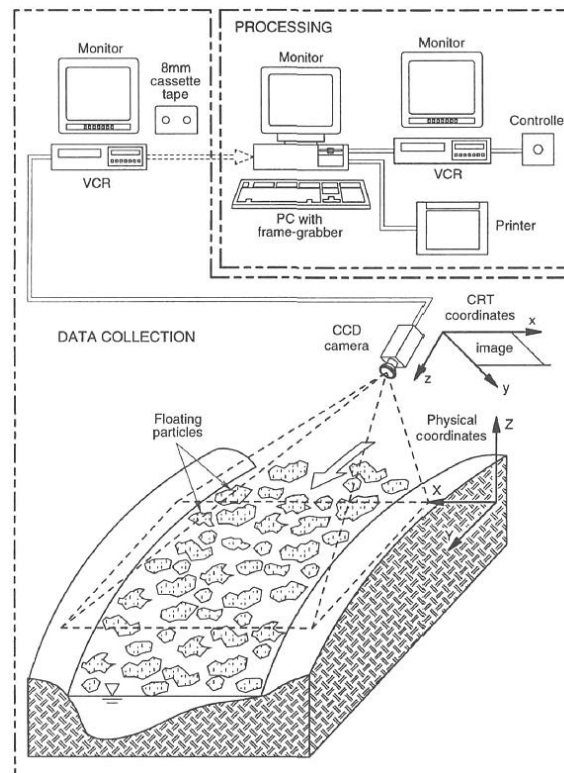


**Figure 5.** Schematic diagram of the LSPIV image acquisition and processing components. From [26].

In [22], the technique is applied to videos recorded with instrumented cameras and they have minimal disturbances of the video frames. However, the videos of the mudflow of the El Tejado ravine present sudden movements and disturbances in the frames. Most of the videos are amateur, that is, recorded from cell phones by residents of the affected sectors, and, therefore, we have low-resolution videos that present slight movements of the camera to different sides. That generated distortion of the frames and blurring of the recorded scene, which made its analysis difficult and presented a certain degree of uncertainty in the results. Instead, it can be considered that it has obtained a good result.

3.2. Sedimentological Approach

Between the dates February 1 and April 22, 2022, four field trips were carried out in the areas affected by the January 31, 2022 mudflow in the sectors: La Comuna, La Gasca, Pambachupa Park, and 10 de América, 10 de Agosto, Cristobal Colón, and 6 de Diciembre Avenues, and also on the streets that cross these Avenues.





Data on deposit and sediment thickness, flood footprint, extension, and flow characteristics were recorded. Data on the slopes of the streets were also recorded to understand how this factor, added to the presence of different urban structures such as sidewalks, speed breakers, or flower beds, influenced the flow behavior.

For the textural and compositional analysis three samples were used (see Figure 3 for localization): M1 taken on Núñez de Bonilla Street (UTM: 777773.49E, 9978480.40S), M2 collected on Alonso de Mercadillo Street (UTM: 778525.36E, 9977973.40S) and M3 in the Atacames Passage (UTM: 777121.03E, 9978310.59S). It can be considered that M1 and M2 samples were obtained from sediment stuck on walls and M3 sample was recollected from fresh sediment.









Once the samples were homogenized and quartered, they were sieved to obtain a granulometric distribution of the components [27]. The histograms and statistical parameters were created, which include mean, median, mode, standard deviation, skewness coefficient, and kurtosis.

The material retained on the sieves was again quartered for visual recognition using a binocular magnifying glass. The components were grouped into four main classes and their respective subclasses (Table 2). Additionally, the characteristics of the clasts were recorded, such as roundness, sphericity, shape, and composition.

**Table 2.** Classes and subclasses for mudflow sedimentary components classification. From [17].

Class	Subclass	Reference image
Organic material	Branches, leaves, bark and tree fragments	
Anthropic material	Concrete, brick, paper, plastic, coal	
Lithic fragments	Light gray lithic fragments	
	Dark gray lithic fragments	



Mineral fragments	Reddish lithic fragments	
	Pumice	
	Plagioclase	
	Amphibole	
	Volcanic glass	
	Magnetite	
Undefined	Quartz	
	Aggregates with plastic	

4. Results

The observation and the cartography of the sediments spread in the affected area determined that the mudflow traveled a distance of 3.2 km from the La Comuna sector (sewage collector area) to 6 de Diciembre Avenue (in a straight-line considered) [19].

It changed its direction to every crossing street, maintaining a NW-SE main flow meaning (Figure 3).

From considering the behavior of the flow, it was divided into four zones for this analysis (Figure 6):

- 1. The Direct Impact Zone (collector area and surroundings)
- 2. Northern Axis (along the Núñez de Bonilla Street)
- 3. The Southern Axis (along the La Gasca Avenue)
- 4. The Distal Area (between América and 6 de Diciembre avenues)

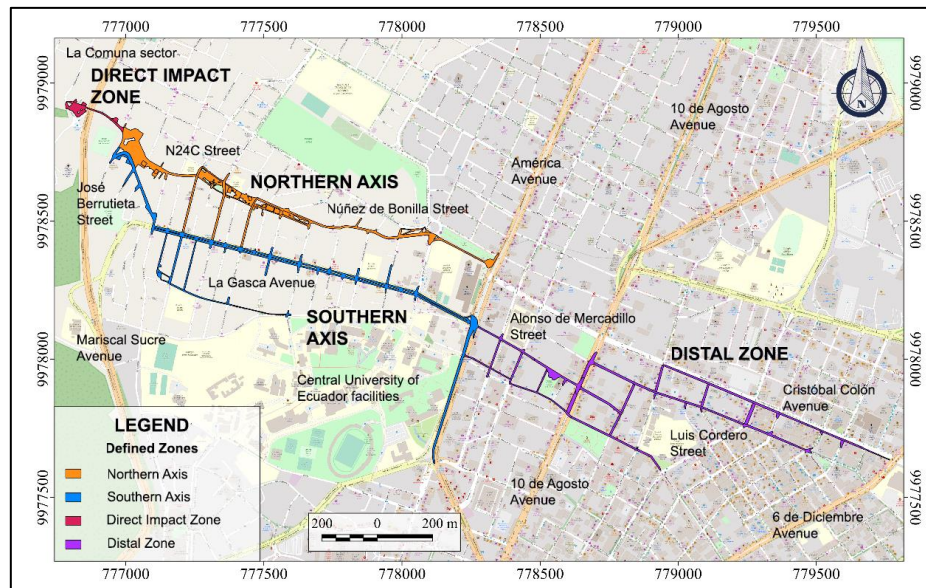


**Figure 6.** Map with the sections' classification according to the mudflows' behavior on January 31, 2022. Modified from [20] using a base-map from Spanish version of [13].

The North and South axes cannot be considered the same section because their behaviors (such as flow dynamic and deposition materials) are different and are the result of the influence of anthropic elements (urban waste materials, street design, and structure, sections), direction, and general topographical inclination. It can be noticed that Pambachupa Park plays a special role in the distribution of the mudflow along the Northern Axis, and made some changes in the distribution of flood, which eroded the North Axis during its development. At the same time, the Southern Axis presents a more straight-line shape and fewer constrained conditions.

About the multimedia material, a total of 65 videos documenting the mudflow's development were identified and georeferenced. However, only four videos had a time record that allowed the start time and progress to be established (Table 1). These times have a high degree of uncertainty given that there is no information on the accuracy of the equipment that recorded the event (Figure 7) [20].

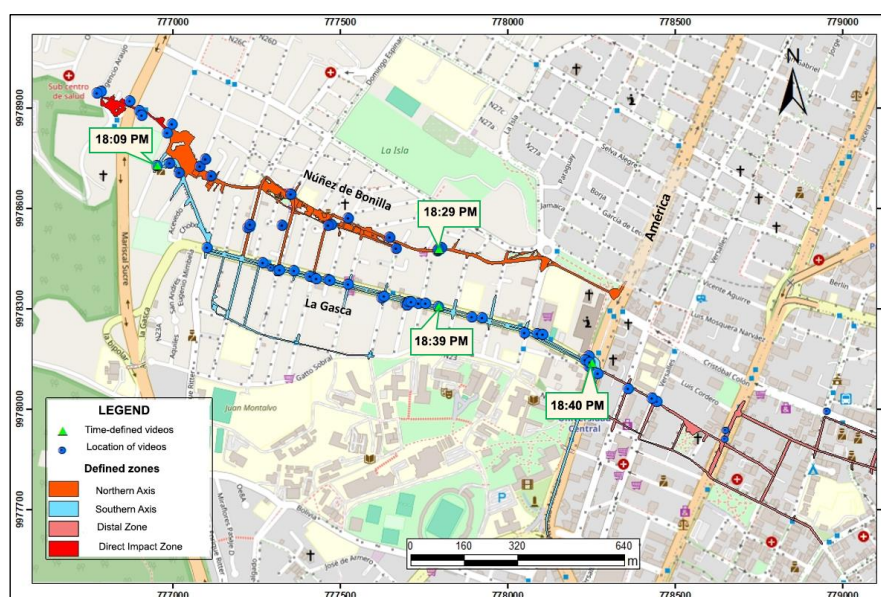


**Figure 7.** Spatial and temporal location map of videos of the development of the mudflow on January 31, 2022. Modified from [20] using a base-map from Spanish version of [13].

#### 4.1. Direct Impact Zone

The Direct Impact area corresponds to the La Comuna sector, where the flow occupies the streets Fulgencio Araujo, Padre Semanate, and José Berrutieta before entering the Belisario Quevedo volleyball sports field (Figure 8). At the intersection of José Berrutieta Street with Antonio de Herrera Street the flow was split into two branches.

That flow presented a turbulent behavior, and those zones were considered an erosional area due to the street slopes, between 5° and 12°. The observed deposit had a maximum thickness of 1 cm, and the flood footprint reached 2 m on building walls.

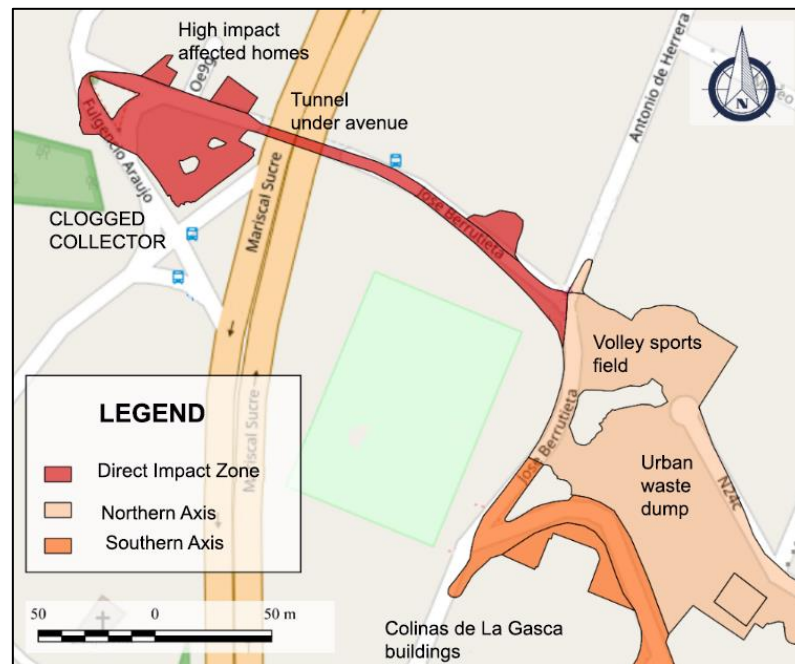


**Figure 8.** A detail of the areas of direct impact in the La Comuna sector. Modified from [17] using a base-map from Spanish version of [13].

The analysis of the multimedia images and footage determined that only two videos were helpful for the analysis of the flow behavior [20]. The entrance of the mudflow to the urban area through José Berrutieta Street could be identified, and it was characterized as a continuous flow with a high sediment load and high energy (Figure 9A). The estimated surface velocity was 4 to 5 m/s by mapping specific frame points.

It must be emphasized that the flow showed a high carrying capacity, evidenced by the damage to the buildings in the sector and the height of the flood footprint [17]. A change in flow behavior was also determined by the increase in speed and energy caused by its passage through a tunnel under Mariscal Sucre Avenue (approximately 6.0 m in diameter; Figure 9B). That was evidenced in the dragged and transported vehicles, tree trunks (up to 3 m long), mesh fences, and 1.5 m in size rubble.

According to the Municipality of Quito [14], in the evaluation of affected properties before the flow entering the tunnel, six buildings were established still as habitable homes; two non-habitable properties on the first floor and one property had damage to the structure and other structural pathologies (Figure 9B). The three homes most affected were those that received the direct impact of the flow upon entering the street. Meanwhile, to the east of the tunnel (after the passage of the flow), the properties were classified as three habitable homes and four non-habitable homes on the first floor; that is, even though the home did not present structural damage, the first floor was affected by the entry of flow and debris.





**Figure 9.** (A) The video frame shows the flow entering José Berrutieta Street through the tunnel and the flow direction from the existing clogged collector (right side of the picture behind the wall) [20]. (B) Damage and affected homes west of the La Comuna and the tunnel section (see vehicle size for scale) under Mariscal Sucre Avenue [17].

#### 4.2. Northern Axis

This axis follows a straight path according to the input direction, and upon reaching the volleyball sports field, the flow destroyed its structures and carried away about 50 people [28]. Before that area, the mudflow had been divided into the branches mentioned: the one that continued along N24C Street (the north side) and the other along José Berrutieta Street until it reached La Gasca Avenue (south side). The Northern Axis (Figure 10) spanned from the volleyball sports field, along N24C and Núñez de Bonilla main streets (NW-SE direction) up to it reached América Avenue, where it ends. It also flowed through the transversal streets: Francisco Lizarazu, Domingo Espinar, and Fernández de Recalde (mentioned those from west to east) [19].

In this section, the flow presented a different behavior than the previous flow and the Southern Axis because, to the east of the volleyball sports field, there was a  $35^\circ$  inclination slope and 8 m high from the first step to the down next level. Under the volley field, there was a stepped waste dump with material of unconsolidated urban origin (presence of construction remains, pipes, plastics, and others) of  $2100 \text{ m}^2$  ( $\sim 6000 \text{ m}^3$  in volume) approximately (Figure 11). That slope caused a cascade effect

where the direct impact of the flow on the deposit has an erosive process that allowed the Northern Axis flow to be enriched with that material (sediments, debris and garbage) [19].

According to [17], on N24C Street, a sedimentary deposit with an average thickness of 7 cm and 40 to 20 cm was found on the ground floors of the buildings located east of the waste dump that were directly impacted. [20] points out that on this street, the flow had a high-energy turbulent and erosive flow behavior that destroyed the structures (enclosing walls) of several buildings and showed high load capacity by dragging cars, tree trunks up to 2.5 m, and debris from 10 cm to 200 cm in diameter. An analysis of several frames estimated a surface speed between 10 and 11 m/s.

The damage in the east area of the waste dump is summarized in homes with total collapse, a high degree of structural damage, and non-habitable homes on the street elevation ground [14]. Therefore, the waste dump and the change in the main slope ( $10^\circ$  inclination) influenced the variation in flow behavior (higher speed and energy) that determined a high degree of impact on the homes with a greater exposure (by the closeness) to this diverse material accumulation area.

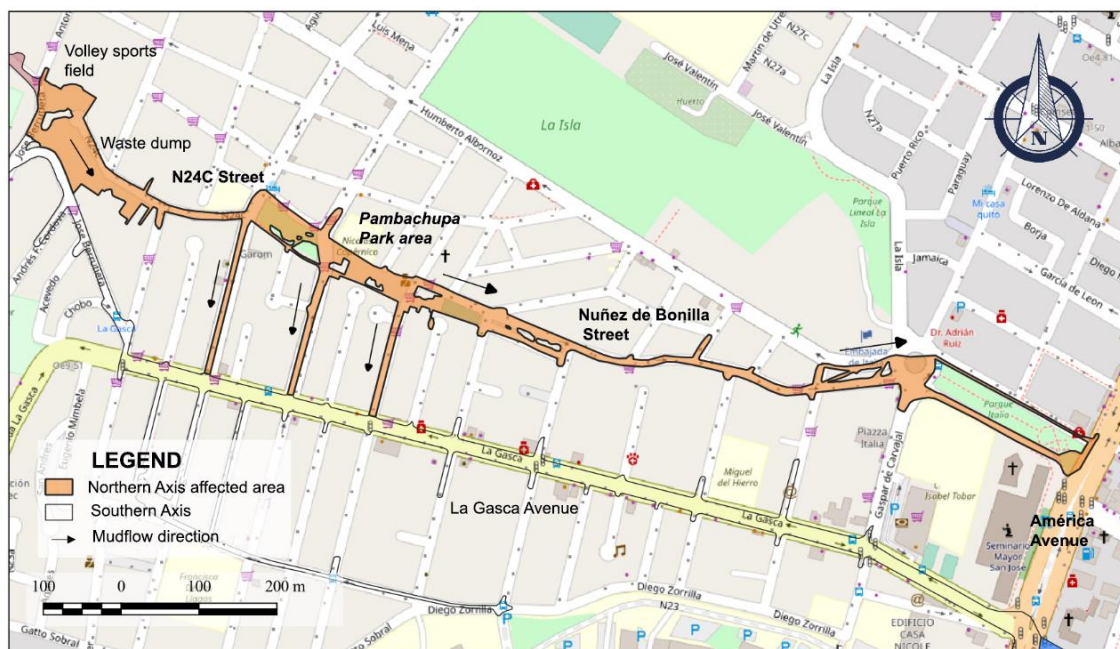


**Figure 10.** Map showing the total flow path of the North Axis. Modified from [17] using a base-map from Spanish version of [13].

To the east of N24C street, the flow entered the Pambachupa Park, a linear area of 440 m long and 30 meters wide approximately (Figure 10), characterized by green fields on stepped terraces with a main inclination of  $4^\circ$  towards the southeast. The presence of two buildings (a communal house and a community police unit) inside the park generated artificial barriers where the flow collided. It allowed a part of the flow to enter through transversal streets from the park (Domingo Espinar and Fernández de Recalde streets). It was determined that the entrance through Francisco Lizarazu Street (at the upper head of the park) was the product of an inclination towards the south (Figure 12). According to [20], the surface speed, calculated from the surveillance camera frames on Domingo Espinar Street (where it has a  $1^\circ$  to  $2^\circ$  inclination), was less than 2 m/s. In addition, the mudflow flowed with a dense behavior able to transport trees larger than 1 m and some cars.

The flow that advanced through the transversal streets ended at La Gasca Avenue, feeding the flow that advanced along the Southern Axis.



**Figure 11.** The volleyball sports field and the stepped urban waste dump are at the beginning of the so-called North Axis and N24C Street. Modified from [29].

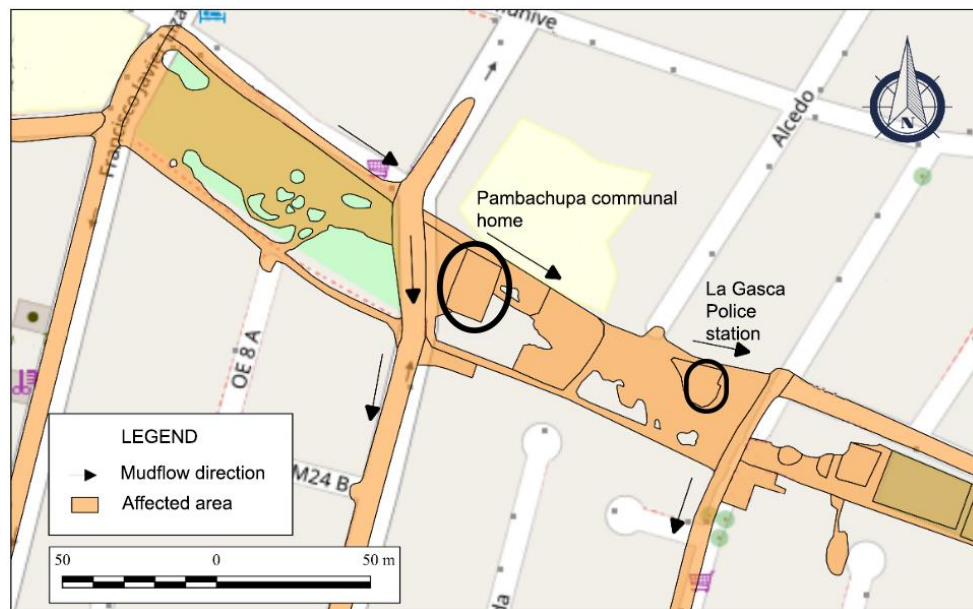


**Figure 12.** A detail of the Figure 10 map showing the Pambachupa Park area. Modified from [17] using a base-map from Spanish version of [13].

The arrival time of the flow to the area located at approximately 1.05 km from the clogged collector was 6:29 PM, obtained from the analysis of the video of a surveillance camera located in the Núñez de Bonilla Street, the east of Pambachupa Park (UTM: 7770811.9E, 9978725.6S). That local time is highly uncertain due to the lack of information about its calibration.

Furthermore, it was established that the flow behavior was waved. It was characterized by a main front and smaller secondary waves, which can still carry medium-sized tree trunks, cars, and garbage containers. Using the Fudaa-LSPIV 1.9.2 software [21], an average velocity of 3.28 m/s and a flow rate of 4.89 m<sup>3</sup>/s were calculated.

The behavior of waves was evidenced again through videos up to 1.3 km from the collector, in an area with 2.5° inclination where the deposited material has shown a thickness of 5 cm associated with organic material (trunks, branches up to 30 cm and different kind of chips), garbage containers, and unclassified garbage.



#### 4.3. Southern Axis

The Southern Axis was defined as spreading along José Berrutieta Street through La Gasca and América Avenues, entering the transversal streets of Atacames, Francisco Javier Lizarazu, and Romualdo Navarro. That flow fed a new split branch that crossed from west to east along Diego Zorrilla Street for approximately 500 meters. This branch constitutes the southern boundary of the affected area and is located approximately 400 m wide to the south of the Northern Axis, being the most widespread (Figure 13).

In the area where the main axes were divided, it could be observed that the flow moved south along José Berrutieta Street, forming a kind of barricade of tree trunks and vehicles that prevented its entry into a residential complex, the Colinas de La Gasca urbanization (Figure 14) and continued its journey with heading southeast, along the same street, until it reached La Gasca Avenue.

A video recorded by a private security camera located on José Berrutieta Street (UTM: 776953.9E, 9978729.3S) indicates that the start of the event south of the volleyball sports field and prior to the formation of the barricade was at 6:09 PM (with also a high degree of uncertainty because there is no information about the camera's time calibration). In addition, it can be seen that the flow advance has a high energy, evidenced by the towing capacity of several vehicles (which was part of the barricade at the entrance to the habitational complex; see Figure 14A,B).

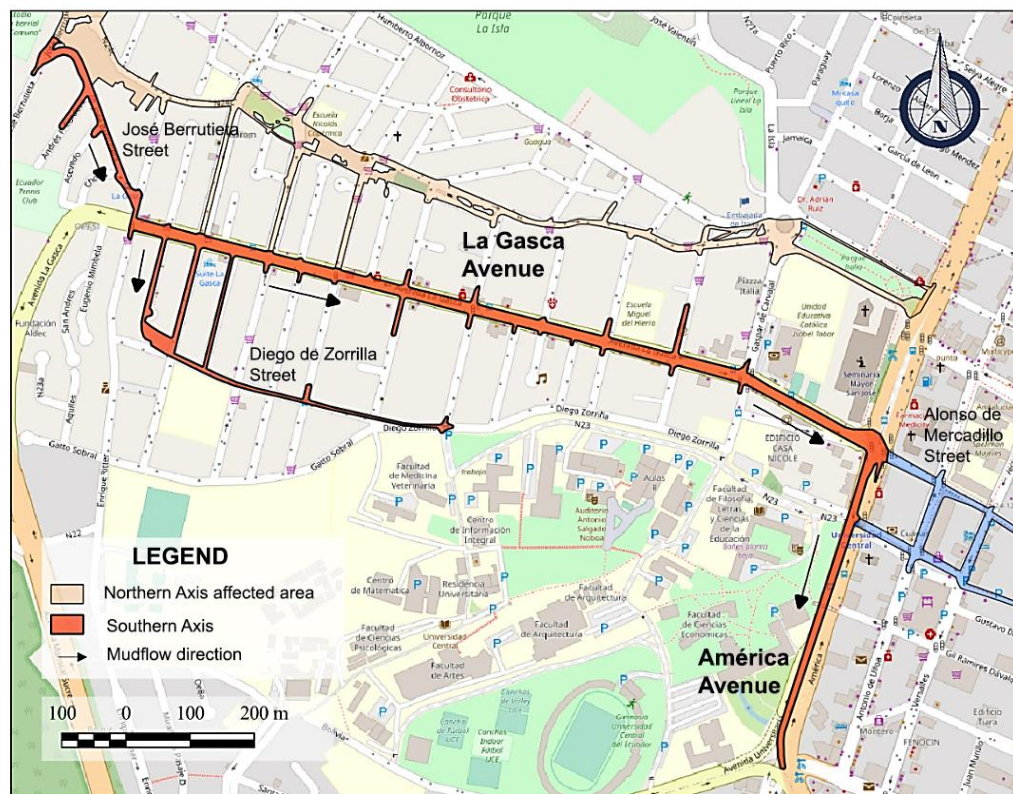


**Figure 13.** Southern Axis affectation area. Modified from [17] using a base-map from Spanish version of [13].

It can be observed that on La Gasca Avenue, the flow still had a high load capacity. The videos and pictures show the transporting of cars, garbage containers, several sizes of debris, and tree trunks of up to 2.5 meters. The average thickness of the deposit along that avenue was 5 cm. In this area, the wave's behavior was changed because the largest fraction of material was deposited (up to 3.0 m). At the same time, the aqueous flow and finest parts overflowed the accumulated material, generating a new waved flux phenomenon [17].

Additionally, it is noted that the footprint of the maximum flood left on the walls of La Gasca Avenue was approximately 35 cm. [20] points out that the analysis of the videos allowed the flow to

be characterized by arrhythmic (non-periodic) waves in which the front, the body, and the tail of laminar layers could be identified. The surface velocity calculated with the support of the video frames was 5 to 6 m/s in an area 430 m away from the flow entrance through La Gasca Avenue (where it has a slope of  $5^\circ$ ). Recording footage obtained from the ECU-911 security cameras, approximately 730 m from the top entrance of the flow to La Gasca Avenue, indicates a record of the event passing at 6:39 PM local time (the front of the flow is not recorded). The time from that kind of records can be considered with less uncertainty than others (official cameras against private ones). In this video record, intermittent waves are observed in all areas ( $3^\circ$  inclination), and the analysis of the frames allowed us to estimate a speed of 3 to 4 m/s.

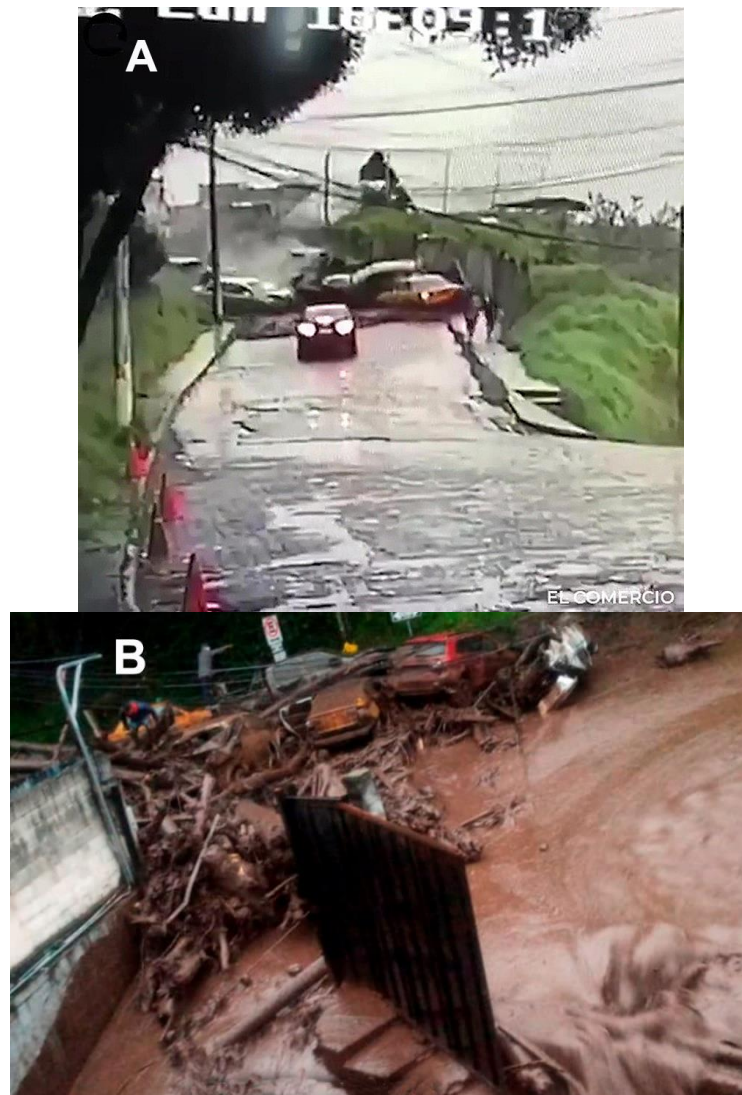


**Figure 14.** Barricade formed by tree trunks and vehicles on José Berrutieta Street. (A) Obtained from [30]. (B) Picture obtained from a private security camera (80-CJB), frame: 444/613 [29].

The flow reached the intersection with América Avenue, approximately 1.2 km from the entrance to La Gasca Avenue, at 6:38 PM (local time). During 30 minutes, the flow developed with an average of four waves per minute [17]. At the intersection with América Avenue, it was observed that the deposit had a thickness of 5.6 cm and was made up of organic matter (trunks up to 1 m long and branches) and garbage with the lithic sedimentary deposit made up of sand.

#### 4.4. Distal Area

The end of Southern Axis flow was América Avenue, and from there, it continues the advance along Alonso de Mercadillo Street just now in the Distal Area. That also affected the Cristóbal Colón



Avenue and the transversal streets (all in NW-SE direction) until the main avenues, such as 10 de Agosto and 6 de Diciembre Avenues, which have NE-SW directions (Figure 15). During the information gathering on February 2, 2022, it was determined that the deposit in this area was made up of primary and remobilized material (lithic sediments), as a product of the artificial washing of La Gasca Avenue (for removing the mud).

The average thickness was 5 cm, except for 10 de Agosto Avenue and its intersection with Alonso de Mercadillo Street, where a large amount of material was accumulated, covering a total area of 2937 m<sup>2</sup> with an average thickness of 54.9 cm [17]. The largest accumulation area was located near Santa Clara de Millán Park, approximately 2.0 km from the clogged collector (Direct Impact zone) and in a plain area with no slope (0°). The deposit comprises sandy silt with organic matter (branches, chips, and 50.0 cm pieces of tree trunks) and garbage.

That change in thickness sedimentation behavior is because, in this area, there was a change in slope from 5° that gradually passes to 0° and the influence of vial structures (street steps and sidewalks approximately 30 cm high from street pavement elevation). Those conditions acted as barriers to the advance of the mud flow towards the east and became deposit areas for most sediment. In addition, this caused the flow to be driven to 10 de Agosto Avenue and advanced through Luis Cordero, Alonso de Mercadillo, and Ignacio de Veintimilla streets. The most extended branch is the one located to the north, over Luis Cordero Street, which, in its advance, entered through Cristóbal Colón Avenue until the intersection with 6 de Diciembre Avenue. That was 3.2 km from the collector.

According to the analysis of the multimedia material, the flow advances through the Distal Zone as a flood of water with low sediment load, speed, and energy [20].

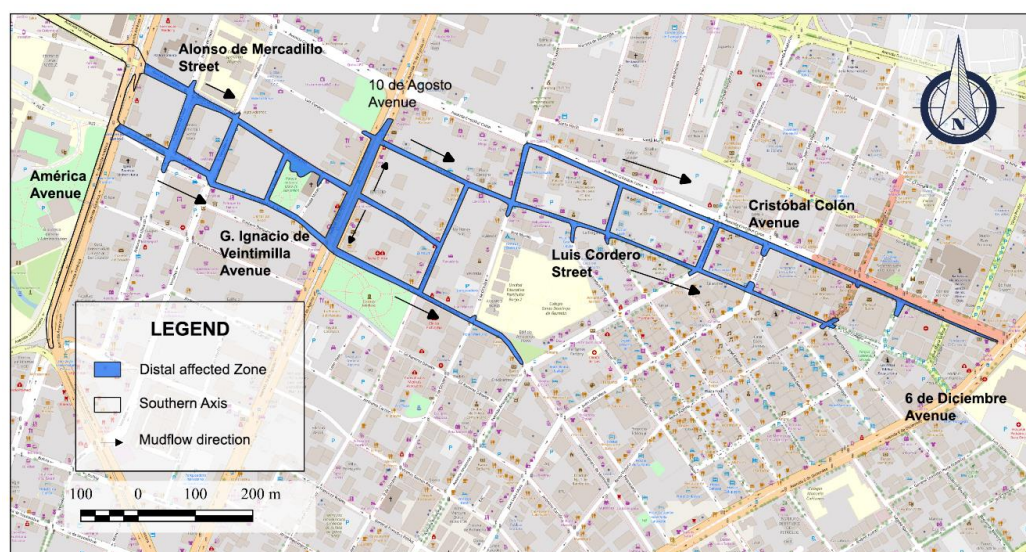


**Figure 15.** Distal Zone of affectation. Modified from [17] using a base-map from Spanish version of [13].

The furthest deposit was identified approximately 3.0 km from the collector on Cristóbal Colón Avenue, which is made up of fine sand and has less presence of organic matter (tree bark, leaves, small branches, and vegetation) and garbage. The deposit was less than 1 cm thick (Figure 16).

It was considered that the total area of the deposit in the affected zones was 100 000.9 m<sup>2</sup>. That was used to calculate the total volume of the mudflow deposit. The thickness varied in the different branches according to the inclination of the streets and flow behavior (erosive or depositional phase). In summary, the thickness on the Northern Axis was 1 to 40 cm, the Southern Axis between 5 and 10 cm, and the Distal Zone between 1 to 5 cm, with the accumulation zone of 54.9 cm in the Santa Clara de Millán Park sector. Therefore, the deposit volume was 7 162.77 m<sup>3</sup> [17].

Also, it was considered that the flood footprint presented average values of 90 cm in the direct impact zone and an average of 57 cm in the Northern Axis. On the Southern Axis, it had an average



value of 19 cm, and in the Distal Zone, it reached an average value of 9 cm. So, the flow volume was 46 218.91 m<sup>3</sup>, covering a total area of 122 790.74 m<sup>2</sup>.



**Figure 16.** Deposit-related thickness to the mudflow is located east of the distal zone, approximately 3.1 km from the collector (five cents coin diameter is 21 mm).

4.5. *Sedimenological Patterns*

The result of the sieving of the three collected samples is shown in Table 3. The differences in sample M3 are due to the previous treatment that the sample had for granulometry analysis by hydrometry.

**Table 3.** Results of the sieving of the collected samples.

Sieve #	M1 sample	M2 sample	M3 sample
	Retained weight (gr)	Retained weight (gr)	Retained weight (gr)
4	5.40	18.76	-
10	21.61	25.80	9.03
20	41.82	34.25	-
40	77.18	69.86	26.8
60	60.10	60.35	-
100	62.88	80.22	-
200	45.62	51.34	53.02
End tail	82.50	82.54	-
Total weight	397.11	423.12	88.85

Sample M1 (collected on Núñez de Bonilla Street on the Northern Axis, approximately 1 km from the clogged collector) comprised 8.6% fine gravel (composed by the undefined aggregates) and 91.4% sand. Its central tendency parameters were mode 1.66, median 1.45, and mean 1.45, showing a poor draw (1.52), bias towards coarse components (-0.19), and mesokurtic (1.05). The histogram presents a unimodal distribution with the highest frequency (26.01%) in the medium sand particles (1 and 2 Φ).

Sample M2 (collected on Alonso de Mercadillo Street in the Distal area, approximately 1.9 km from the collector) comprised 13.1% fine gravel (composed by the undefined aggregates) and 86.9% sand. The central tendency parameters were mode 2.37, mean 1.57, and median 1.22, with a poor

draw (1.67), and bias towards thicker and mesokurtic components (1.07). The histogram shows a unimodal distribution (29.81) in fine sand particles (between 2 and 3  $\Phi$ ).

Sample M3 (collected in the Atacames Passage on the Southern Axis, less than 500 m from the collector) comprised 54% sand and 46% silt, corresponding to silty sand. This sample was the only one taken wet, and the drying and sieving processes before carrying out the granulometric analysis destroyed the gravel-sized aggregates found in samples M1 and M2 [17]. The measures of central tendency were mode 2.53, mean 1.42, and median 1.71; poor draw (1.52); bias towards the coarsest particles (-0.16); and very platykurtic (0.65). The histogram shows a unimodal distribution most frequently in sand size (1.3 and 3.9  $\Phi$ ). The sample has 34.64% coarse sand (0.1  $\Phi$ ) and 65.36% fine sand (2.5  $\Phi$ ).

In summary, the material from the waste dump with unconsolidated anthropic deposits located east of the field contaminated the material of samples M1 and M2. Sample M3 was obtained south of the Atacames Passage in the Ritter Park area without the influence of material from the waste dump, so it did not present evidence of contamination, such as anthropic material or aggregates of silty material [17].

The samples generally contained 15.5% organic components, 2.5% anthropic components, 55.0% lithic fragments, and 27.0% mineral fragments. The lithological component comprised pumice clasts, rock fragments of andesitic and dacitic composition, and mineral fragments of quartz, plagioclase, amphibole, and magnetite. The fine gravel-sized aggregates comprised silty material, including plastic remains (Figure 17A). The cohesive nature of these materials favored the formation of clots or flocs due to Van Der Waals forces [31].

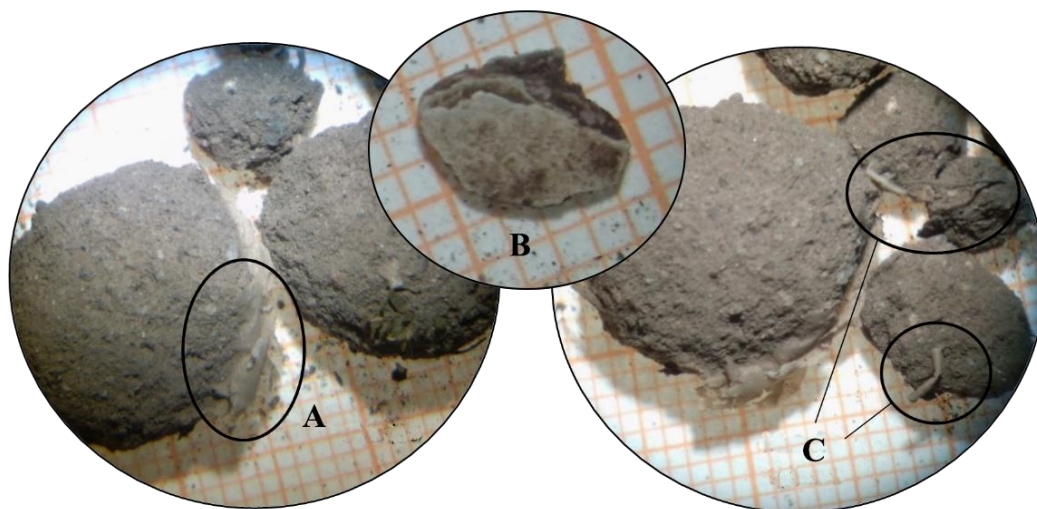


**Figure 17.** Fine gravel-sized silt aggregates in M2 sample (retained particles in sieve #4). (A) Plastic piece. (B) Undefined anthropic material. (C) Organic matter.

## 5. Discussion

The flow on January 31, 2022, is similar to the 1975 event. These include the meteorological conditions due to the occurrence of intense rains in a short period, the erosion of drainage at high levels of the hydrographic basin, and the occurrence of small landslides on the edges of the stream [7].

A strong anthropic influence altered the flow of 2022 due to the presence of limiting structural elements, such as the tunnel and the presence of new constructions and living areas (volleyball court, park, and waste dump) and the constructions on the edge of the Broken. Elements that did not exist in the case of the 1975 flow [7].

The flow behavior has been presented as variable, starting from a turbulent regime in the western area, starting from the collector and then along N24C, Núñez de Bonilla streets, and the upper and middle part of La Gasca Avenue. In these areas, it reached a speed of up to 11 m/s, and

the flow was also characterized by presenting phases of successive waves. This energy decreased towards the eastern zone and was degraded by the intersections between the transversal streets and by the changes in slope (reaching the distal zone where the slope is 0°). The speeds observed in the final zone were less than 4 m/s [32].

With these values and taking into consideration the classification of [33], the mud flow is a small, high-speed event with a water content of 45.67% and a density of 1,547 gr/cm<sup>3</sup>, which classifies it as a flow with enough water to behave like a liquid and a hyper-concentrated flow according to [34] (obtained from M3 sample).

The sediment load has been high in the area of higher elevations, as well as when the flow crosses the waste dump area. In the distal area, this flow behaves as a water compound with fine sediments because the coarser components are deposited in other points, such as the Santa Clara de Millán park area [35].

The stream and drainage area in the 1975 event was in a wild state with native vegetation (shrub and herbaceous) and without eucalyptus plantations and woody trees [7]. In the flow of 2022, the drainage area and the basin of El Tejado were occupied, for the most part, by non-native forest exploitation plantations on its slopes and even near the riverbed (eucalyptus). It also had a significant load of garbage and anthropogenic remains (especially construction) deposited uncontrolled by the city's residents. This garbage accumulation process is believed to have been enhanced during the COVID-19 pandemic period (almost two years of restrictions were suffered in Ecuador) as there was no regular garbage collection [36].

The city's design in the area that was crossed by the flow (direction and inclination of the streets, above all) determined the behavior of the flow and, therefore, the areas of impact and most intense affectation, as indicated in [35]. The layout of the streets and the waterproof materials that cover them (asphalting and concrete) condition the direction and behavior of the flow [11,12,36,37]. For example, the slopes of the main streets and their intersections (avenues) have been fundamental in the flood's path.

The sedimentological characteristics of the flow (pumice, andesites, and dacites) could be assimilated to a lahar type of secondary origin due to both the existing relationship with the drainage area (slopes of the Pichincha volcano) and its rheological behavior [33]. However, it must be highlighted that it is highly anthropogenic-influenced drainage, especially from the interventions of the EPMAFS [16] action projects in the stream (flood control) and the urban occupation of the stream's banks in the collection environment and entrance to the collector. That has resulted in the appearance of a complex mass flow composed of rock blocks, fine lithic material, plant remains, and debris (of anthropic origin). It is unknown if the sewer collector is the correct size or if it is due to the current climatic conditions and the drainage volume from the hydrographic basin, as commented in [35,36].

It has been evident that the presence of plastics and microplastics (detected sizes of 8 to 25 mm) has generated agglomerates (aggregates) of gravel size to soft small boulders (> 10 mm) that cannot be classified in known geological terms. For this reason, they have been classified as undifferentiated.

Social networks have become fundamental tools in this research due to the variety of points of view shown in images and ideas and because of the access to them (free of charge). With their contribution, it has been possible to complete and complement the data from the official recordings (those belonging to the municipality), which have been scarce (only four control and reliability cameras were available) [28–30].

## 6. Conclusions and Recommendations

The obtained data determine that the 2022 flow constitutes a mass-flow movement of small magnitude, and compared to the previous 1975 flow described by Feininger [7], it is seven times smaller, according to data published in the media of the time (we consider that it can be an overestimation). However, the structural damage and loss of life have been more significant on this occasion.

Anthropic conditions have conditioned both the trajectory and behavior of this 2022 flow. On the one hand, the collapse at the entrance of the collector (by tree trunks and stone blocks up to 3 m



in diameter and 7 tons in weight [14]) prevented the accumulating water and sediments from being conducted correctly; on the other hand, the new constructions and the use of the soil in the environment of sewage collector and the surroundings. The less-intervened environment in the 1975 mudflow allowed stone blocks to reach the middle of La Gasca Avenue [7]. It is worth highlighting the importance they have had in the behavior of the flow of the volleyball court and the waste dump, as well as their staggered layout (terracing). In these cases, erosion was generated, enriching the incoming flow with sediments.

The characteristics of the 2022 flow determine the need to define new parameters and conditions of these events in urban or urbanized environments because these areas do not adapt to the parameters of natural environments and environments. In addition, land use and territorial planning must consider the occurrence of these extraordinary events to avoid creating spaces with high human exposure (volleyball court) and the placement of elements that influence the phenomenon's behavior (slag heap and garbage). Streets and buildings constrain the mudflow shape and do not have a typical fan shape of this phenomenon.

The consequences of the pandemic (deposition of garbage in the stream) and the lack of sanitation of the collectors and natural drainage areas concerning this type of special event must be evaluated in the medium term. Also, managing the drainage area is a valuable need [37].

The possible expiration of works that have exceeded the return periods of their construction and whether they respond to the demands related to climate change and the city's urban development must also be analyzed [38,39].

On the other hand, the different recordings and images consulted are of low to medium quality and available through the network. However, education of the population could be considered so that these graphic documents are recorded with the best possible quality for later use in this type of assessment and the improvement of the municipal video surveillance system.

**Author Contributions:** Conceptualization, L.T., E. I., and L. P.; methodology, L. T., E. I., F. V. and L. P.; software, A. M., R. C., O. A.-P. and N. R.; validation, L. T., E. I., F. J. T. E., and L. P.; formal analysis, F. J. T. E., and O. A.-P.; investigation, L. T., R. C., N. R., S. S. and L. P.; resources, R. C., S. S., and N. R.; data curation, F. J. T. E., L. T., L. P., E. I., and O. A.-P.; writing—original draft preparation, L. T., and O. A.-P.; writing—review and editing, O. A.-P., F. V. and F. J. T. E.; visualization, A. M.; supervision, F. J. T. E., and O. A.-P. All authors have read and agreed to the published version of the manuscript.

**Funding:** This research received no external funding.

**Data Availability Statement:** The supporting information and managed data can be available under requested using the corresponding email.

**Acknowledgments:** The support provided by the Central University of Ecuador (UCE) authorities to the students and professors of the Faculty of Geology, Mining, Petroleum, and Environmental Engineering and the Geology Department for collecting and managing the information in the affected area is appreciated. The granulometric analyses were carried out thanks to the help of the laboratories of the Faculty of Engineering and Applied Sciences of the UCE. The analysis of the behavior of the mud flow was thanks to the access provided to the videos from the surveillance cameras by the ECU-911 Integrated Security System. We also want to thank the Secretaría de Seguridad de Gobernabilidad of MDQ, who supports us with the DEM of the affected area, and the historian Rafael Racines for his comments. We also would like to thank the anonymous reviewers and the academic editor whose comments improved this manuscript.

**Conflicts of Interest:** The authors declare no conflicts of interest. Facebook (www.facebook.com), TikTok (www.tiktok.com), Instagram (www.instagram.com), YouTube (www.youtube.com), Twitter/X (www.twuitter.com) and Google Maps (www.maps.google.com) are trademarks.

## References

1. Hutter, K.; Svendsen, B.; Rickenmann, D. Debris flow modeling: A review. *Continuum Mech. Thermodyn.* **1994**, *8*, pp. 1–35. <https://doi.org/10.1007/BF01175749>
2. Greco, M.; Di Cristo, C.; Iervolino, M. Numerical simulation of mud-flows impacting structures. *Journal of Mountain Science* **2019**, *16*(2). <https://doi.org/10.1007/s11629-018-5279-5>

3. Takahashi, T. Debris Flow: Mechanics, Prediction and Countermeasures. Taylor and Francis, New York, USA, 2007
4. Alvarado, A.; Audin, L.; Nocquet, J. M.; Jaillard, E.; Mothes, P.; Jarrín, P.; Segovia, M.; Rolandone, F.; Cisneros, D. Partitioning of oblique convergence in the Northern Andes subduction zone: Migration history and the present-day boundary of the North Andean Sliver in Ecuador. *Tectonics* **2016**, *35*(5), 1048–1065. <https://doi.org/10.1002/2016TC004117>
5. Zevallos, O. Ocupación de laderas: Incremento del riesgo por degradación ambiental urbana en Quito, Ecuador. In *Ciudades en riesgo. Degradación ambiental, riesgos urbanos y desastres*. M.A. Fernández Ed., ITDG/LA RED, Red de Estudios Sociales en Prevención de Desastres en América Latina. Quito, Ecuador, 1996; pp. 2-11 <https://www.desenredando.org/> (accessed on 18 April 2023)
6. Fernández, M. A. Zonificación de amenazas naturales y reglamentación urbana en Quito, Ecuador. In *Navegando entre brumas. La aplicación de los sistemas de información geográfico al análisis de riesgos en América Latina*. A. Maskrey Ed., ITDG/LA RED, Red de Estudios Sociales en Prevención de Desastres en América Latina. Quito, Ecuador, 1998; p. 4-36; <http://www.funsepa.net/soluciones/pubs/MTU2.pdf> (accessed on 21 January 2023)
7. Feininger, T. El flujo de escombros en La Gasca. Un informe científico. *Boletín de la Sección Nacional del Ecuador IPGH* **1976**, Volume 5-6, pp. 5-6
8. Vidal, X.; Burgos, L.; Zevallos, O. Protection and environmental restoration of the slopes of Pichincha in Quito, Ecuador. In *Water and Cities in Latin America. Challenges for Sustainable Development*, 1st ed.; Aguilar-Barajas Ed., Taylor & Francis Group, COUNTRY, London, 2015; pp. 173–188 <https://doi.org/10.4324/9781315848440>
9. EPMAPS Informe evento 31 de enero de 2022. Municipio de Quito, Internal report, 2022
10. Fernández, M. El medio físico de Quito: sus limitaciones y su incidencia en la adaptación del hombre. Quito, 1990
11. Bracchi, P.; Torrijo, F.J.; Boix, A.; Cabrera, M.C.; Giordanelli, D. Urban and hydrogeological alert on the morphoclimatic risk affecting Quito's world heritage. In *The International Archives of the Photogrammetry, Remote Sensing and Spatial Information Sciences, HERITAGE2020 (3DPast | RISK-Terra) International Conference*, 9–12 September 2020, Valencia, Spain. Volume XLIV-M-1-2020, 2020, pp. 825-632 <https://doi.org/10.5194/isprs-archives-XLIV-M-1-2020-825-2020>
12. Trizio, F.; Garzón-Roca, J.; Eguibar, M.Á.; Bracchi, P.; Torrijo, F.J. Above the Ravines: Flood Vulnerability Assessment of Earthen Architectural Heritage in Quito (Ecuador). *Appl. Sci.* **2022**, *12*, 11932. <https://doi.org/10.3390/app122311932>
13. Google Maps [www.maps.google.com](http://www.maps.google.com) (accessed on 2 December 2023)
14. Dirección Metropolitana de Gestión de Riesgos. Secretaría General de Seguridad y Gobernabilidad. Aluvión Sector La Comuna y La Gasca. Headquarters Report, Quito, 2022
15. Servicio Nacional de Gestión de Riesgos y Emergencias. Dirección de Monitoreo de Eventos Adversos. Informe 001—Aluvión Quito. Report, 2022 <https://www.gestionderiesgos.gob.ec/wp-content/uploads/2022/02/Informe-de-Situacion-001-Aluvion-Quito-10202022-9h00-2.pdf> (accessed on 21 March 2022)
16. Epmaps - Agua de Quito [X: @aguadequito]. Liberamos la primera rejilla de la estructura de captación que en la Quebrada El Tejado. Con el desalojo del material acumulado el agua empezó a desfogar por el colector principal. Quito, 2022. <https://t.co/2S7RggKWnG> [X] <https://twitter.com/aguadequito/status/1489299821022306309/photo/2> (accessed on 2 March 2022)
17. Rondal, N. Caracterización del depósito del flujo de lodo de la quebrada El Tejado, Quito, 31 de enero de 2022. Bachelor thesis. Universidad Central del Ecuador, Quito, 2022. <https://www.dspace.uce.edu.ec/entities/publication/1da90328-1998-4eee-b155-c20bb39f5d39> (accessed on 12 July 2022)
18. SNGRE - Dirección de Monitoreo de Eventos Adversos. Informe Nro. 11—Aluvión. Report, Quito, 2022
19. Universidad Central del Ecuador. Análisis preliminar del flujo de lodos de la quebrada El Tejado. Report, Quito, 2022
20. Cañar, R. Propuesta metodológica para análisis de aluviones en entornos urbanos mediante material multimedia. Caso de estudio: aluvión de la quebrada El Tejado, Quito, 31 de enero 2022. Bachelor thesis. Universidad Central del Ecuador, Quito, 2024. (unpublished work)
21. Le Coz, J.; Jodeau, M.; Hauet, A.; Marchand, B.; Le Boursicaud, R. Image-based velocity and discharge measurements in field and laboratory river engineering studies using the free FUDAA-LSPIV software. *River Flow* 03/09/2014-05/09/2014, Lausanne, Switzerland, 2014. 7 p. <https://riverhydraulics.inrae.fr/en/tools/measurement-software/fudaa-lspiv-2/>
22. Arattano, M; Grattoni, P. Using a fixed video camera to measure debris-flow surface velocity. In *Second International Conference on Debris-flow Hazard Mitigation Mechanics, Prediction, and Assessment*, Taipei, Taiwan, 16-18 August 2000, pp. 273–281 <http://www.cnr.it/prodotto/i/249666>

23. Arattano, M.; Marchi, L. Video-derived velocity distribution along a debris flow surge, *Physics and Chemistry of the Earth, Part B: Hydrology, Oceans and Atmosphere*, **2000**, 25(9) [https://doi.org/10.1016/S1464-1909\(00\)00101-5](https://doi.org/10.1016/S1464-1909(00)00101-5)
24. Le Boursicaud, R.; Penard, L.; Hauet, A.; Thollet, F.; Le Coz, J. Gauging extreme floods on YouTube: application of LSPIV to home movies for the post-event determination of stream discharges, *Hydrological Processes*, **2015**, 30(1), pp. 90-105, <https://doi.org/10.1002/hyp.10532>
25. Theule, J.; Crema, J.; Marchi, L.; Cavalli, M.; Comiti, F. Exploiting LSPIV to assess debris flow velocities in the field. *Nat. Hazards Earth Syst. Sci.*, **2018**, 18, pp. 1–13 <https://doi.org/10.5194/nhess-18-1-2018>
26. Fujita, I.; Muste, M.; Kruger, A. Large-scale particle image velocimetry for flow analysis in hydraulic engineering applications *Journal of Hydraulic Research*, **1998**, 36(3), pp. 397–414. <https://doi.org/10.1080/00221689809498626>
27. ASTM, Standard Specification for Woven Wire Test Sieve Cloth and Test Sieves E11-22, Book of Standards, 2022, Volume: 14.02, Developed by Subcommittee: E29.01, pp. 12, <https://doi.org/10.1520/E0011-22>
28. Radio Pichincha Obtained from “Situación en La Comuna y La Gasca, tras aluvión” <https://www.facebook.com/PichinchaRadio/videos/696725658415957/> (accessed on 2 February 2022).
29. El Comercio Especiales El Comercio, Aluvión en La Gasca. El Comercio. Obtained from <https://especiales.elcomercio.com/2022/02/aluvion-la-gasca-galeria-donaciones-mapa/#galeria> (accessed on 5 February 2022).
30. Expresate Morona Santiago Emergencia en Quito por Aluvión. Expresate Morona Santiago. Obtained from [https://www.facebook.com/expresatems/photos/a.218828324850041/4933764863356340/?\\_rdr](https://www.facebook.com/expresatems/photos/a.218828324850041/4933764863356340/?_rdr) (accessed on 31 January 2022)
31. Maggi, F. Flocculation dynamics of cohesive sediment. Ph.D. Thesis, TUDelft University of Technology, Delft, Netherlands, 2005 <http://resolver.tudelft.nl/uuid:0dd37043-d40c-44c3-a87b-741caa10b85e> (accessed on 15 October 2022).
32. Adrian, R.J. Particle-imaging techniques for experimental fluid mechanics *Annu. Rev. Fluid Mech.* **1991**, 23(1), pp. 261-304 <https://doi.org/10.1146/annurev.fluid.23.1.261>
33. Cruden, D. M., Varnes, D.J. Landslide types and processes, *Transportation Research Board, Special Report*, **1996**, 247, pp. 36-75. U.S. National Academy of Sciences
34. Hungr, O.; Evans, S.; Bovis, M.; Hutchinson, J. (2001). Review of the classification of landslides of the flow type. *Environmental and Engineering Geoscience*, **2001**, 7(3), pp. 22-238 <https://doi.org/10.2113/gsegeosci.7.3.221>
35. Karkani, A.; Evelpidou, N.; Tzouxanioti, M.; Petropoulos, A.; Santangelo, N.; Maroukian, H.; Spyrou, E.; Lakidi, L. Flash Flood Susceptibility Evaluation in Human-Affected Areas Using Geomorphological Methods—The Case of 9 August 2020, Euboea, Greece. A GIS-Based Approach. *GeoHazards* **2021**, 2, 366–382. <https://doi.org/10.3390/geohazards2040020>
36. Sierra, A. La política de mitigación de los riesgos en las laderas de Quito: ¿qué vulnerabilidad combatir? *Bulletin de l'Institut français d'études andines*, **2009**, 38 (3) *Vulnerabilidades urbanas en los países andinos (Bolivia, Ecuador, Perú)* <https://doi.org/10.4000/bifea.2421>
37. Lipka, O.N.; Andreeva, A.P.; Shishkina, T.B. Protected Areas as Nature-Based Solutions for Climate Change Adaptation. *Environ. Sci. Proc.* **2023**, 27, 34. <https://doi.org/10.3390/ecas2023-15659>
38. Cerbelaud, A.; Blanchet, G.; Roupioz, L.; Breil, P.; Briottet, X. Mapping Pluvial Flood-Induced Damages with Multi-Sensor Optical Remote Sensing: A Transferable Approach. *Remote Sens.* **2023**, 15, 2361. <https://doi.org/10.3390/rs15092361>
39. Ligong, S.; Sidek, L.M.; Hayder, G.; Mohd Dom, N. Application of Rainfall Threshold for Sediment-Related Disasters in Malaysia: Status, Issues and Challenges. *Water* **2022**, 14, 3212. <https://doi.org/10.3390/w14203212>

**Disclaimer/Publisher's Note:** The statements, opinions and data contained in all publications are solely those of the individual author(s) and contributor(s) and not of MDPI and/or the editor(s). MDPI and/or the editor(s) disclaim responsibility for any injury to people or property resulting from any ideas, methods, instructions or products referred to in the content.